AUTHOR QUERY FORM

ELSEVIER	**Journal: APPGEO** **Article Number: 1995**	**Please e-mail or fax your responses and any corrections to:** **E-mail: corrections.esnl@elsevier.spitech.com** **Fax: +1 619 699 6721**

Dear Author,

Any queries or remarks that have arisen during the processing of your manuscript are listed below and highlighted by flags in the proof. Please check your proof carefully and mark all corrections at the appropriate place in the proof (e.g., by using on-screen annotation in the PDF file) or compile them in a separate list.

For correction or revision of any artwork, please consult http://www.elsevier.com/artworkinstructions.

Any queries or remarks that have arisen during the processing of your manuscript are listed below and highlighted by flags in the proof. Click on the 'Q' link to go to the location in the proof.

Location in article	Query / Remark: click on the Q link to go Please insert your reply or correction at the corresponding line in the proof
Q1	The citation "Salvany 2001" has been changed to match the author name/date in the reference list. Please check here and in subsequent occurrences, and correct if necessary.
Q2	Highlights should consist of 3-5 bullet points (with a maximum of 85 characters per bullet point, including spaces). However, the highlights provided for this item are in paragraph form; thus, they were not captured. Kindly provide the necessary corrections. For more information, please see Guide for Authors.
Q3	The citation "Rodríguez 2008" has been changed to match the author name/date in the reference list. Please check here and in subsequent occurrences, and correct if necessary.
Q4	The citation "Rodríguez 2008" has been changed to match the author name/date in the reference list. Please check here and in subsequent occurrences, and correct if necessary.
Q5	Citation "Torge (2001)" has not been found in the reference list. Please supply full details for this reference.
Q6	The citation "Heiskanen and Moritz, 1969" has been changed to match the author name/date in the reference list. Please check here and in subsequent occurrences, and correct if necessary.
Q7	The citation "Knudsen, 1987" has been changed to match the author name/date in the reference list. Please check here and in subsequent occurrences, and correct if necessary.
Q8	The citation "Carbó et al., 2003" has been changed to match the author name/date in the reference list. Please check here and in subsequent occurrences, and correct if necessary.
Q9	The citation "Carbó et al. 2003" has been changed to match the author name/date in the reference list. Please check here and in subsequent occurrences, and correct if necessary.
Q10	The citation "Carbó et al. 2003" has been changed to match the author name/date in the reference list. Please check here and in subsequent occurrences, and correct if necessary.

Thank you for your assistance.

Journal of Applied Geophysics xxx (2011) xxx–xxx

Contents lists available at ScienceDirect

Journal of Applied Geophysics

journal homepage: www.elsevier.com/locate/jappgeo

A comparison of robust polynomial fitting, global geopotential model and spectral analysis for regional–residual gravity field separation in the Doñana National Park (Spain)

A. Martín [a,*], M.A. Núñez [b], J.A. Gili [b], A.B. Anquela [a]

[a] Dept. Ingeniería Cartográfica, Geodesia y Fotogrametría, Universidad Politécnica de Valencia, C/Camino de Vera s/n, 46520, Valencia, Spain
[b] Dept. Ingeniería del Terreno, Cartográfica y Geofísica, Universidad Politécnica de Cataluña, C/Jordi Girona, Modulo 2, 08034, Barcelona, Spain

ARTICLE INFO

Article history:
Received 17 March 2010
Accepted 30 June 2011
Available online xxxx

Keywords:
Gravimetric survey
Doñana National Park
Regional–residual gravity field separation
Iberia
Potential fields

ABSTRACT

Doñana National Park is a protected area of approximately 500 km^2 located on the SW coast of Spain with singular and interesting ecological and geological features. A gravimetric survey is presented where L&R gravity metres were used in the gravimetric observations with GPS and high-precision levelling positioning. Bouguer gravity anomalies were computed and least squares prediction was used for gross-error detection. Robust polynomial fitting, the recent EGM2008 global geopotential model (complete to degree and order 2159), and spectral analysis were tested for regional–residual gravity field separation. A detailed description of the gravimetric characteristics of the Doñana National Park is presented and the values of residual gravity anomalies were correlated with geological features, where the use of the EGM2008 global geopotential model has revealed an interesting tool for regional–residual gravity field separation. Finally, the interpretation of the results is justified by the well-known geological aspects of the park, but some modifications in the boundaries of the different geological features are needed in order to fit the modelled gravity with the residual gravity anomalies in the two cross-sections analysed.

Contents

1. Introduction

Doñana National Park is a protected area because of its ecological diversity and because it is one of the last wetlands in the Iberian Peninsula. It is located on the SW coast of Spain and has an approximate extension of 500 km^2. Practically half of this area is covered by water throughout most of the year. The National Park is directly adjacent to a Natural Park and a Biological Reserve, which bring the protected area up to 1000 km^2 (Fig. 1). It has one of the Iberian Peninsula's great geoid gradients (Núñez et al., 2008) due to its peculiar geological characteristics, making it an interesting area for geological, geodesic, geophysical

* Corresponding author. Tel.: +34 96 3877007; fax: +34 96 3877557.
E-mail address: aemartin@upvnet.upv.es (A. Martín).

0926-9851/$ – see front matter
doi:10.1016/j.jappgeo.2011.06.037

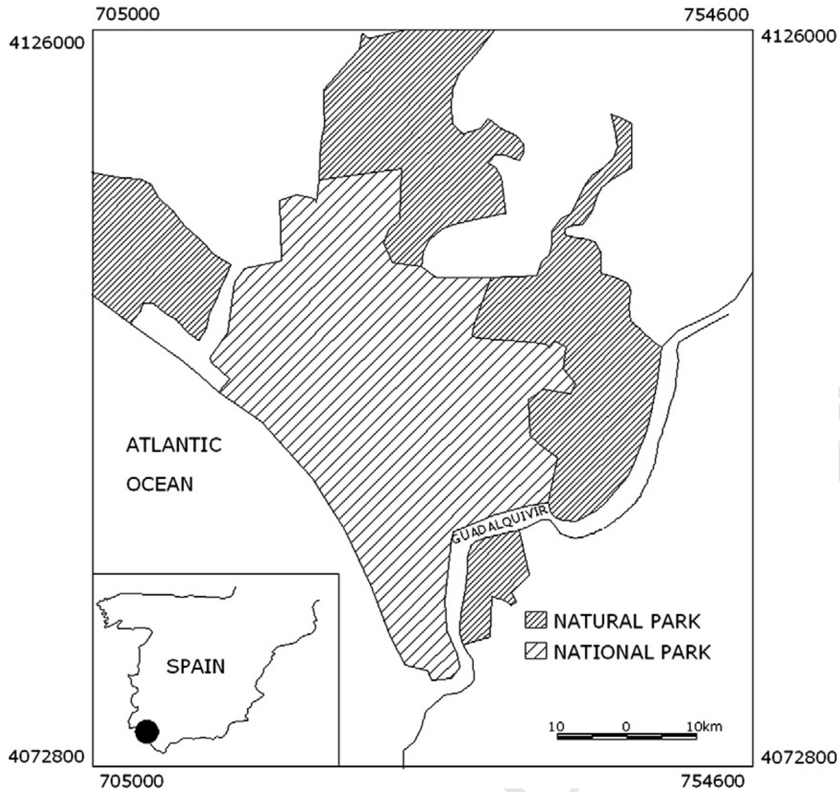

Fig. 1. Doñana Natural and National Park limits. UTM 29 N coordinates. GRS80 reference ellipsoid.

and hydrogeological research. In this regard, gravimetric surveys are a useful tool to study and model distributions of subsurface masses and tectonic features (Torge, 1989). A separation between residual and regional gravimetric components is needed to differentiate between anomalies from local, near surface masses (which are of interest in this kind of studies) and those arising from larger and deeper structures (Dobrin and Savit, 1988; Sharma, 1997).

Results from three different methods to separate residual and regional gravimetric components are presented and compared. These methods are robust polynomial fitting, reduction with a global geopotential model and spectral analysis. Finally, a discussion of the results, from a geological point of view, is presented.

2. Geological setting

Doñana National Park is situated in the Guadalquivir basin, which is located in the southern part of the Iberian Peninsula, limited to the North by the palaeozoic massif of Sierra Morena (the southern part of the Iberian Massif) and to the South by the Betic Cordillera (related to the convergent boundary between the African and Eurasian plates). Some disagreements can be found in different publications regarding the age of the sedimentary infill of the Guadalquivir basin, see for example García-Castellanos et al. (2002), but, in general, the Doñana National Park shows the following stratigraphic and geomorphological characteristics (ITGE, 1992,) of Miocene to present sequence, Fig. 2 and Fig. 3:

a) Blue marls (late Miocene and early Pliocene). This formation is the impervious base of the park. The top of the formation, characterised by a smooth slope, descends to the SE with a maximum depth of 250 m in that part of the marshlands, and a shallower depth in the neighbouring area of the Guadalquivir River, Fig. 2.
b) Basal silts (mid-Pliocene). Due to the regression of the early Pliocene, a change in sedimentation took place, leading to a heterogeneous formation in the park subsurface, consisting in clayey and sandy areas rather than silty areas.
c) Basal sands (Plioquaternary). This discordant formation is located on top of the basal silts. It is 10 to 30 m thick in the coastal area, where there is a strong wind influence. This material constitutes the most significant aquifer level due to its imperviousness and its dimensions.
d) Marshlands. The origin of this formation is not quite clear, although it is admitted that, during the upper and mid-Quaternary, the sea gulf existing in the area started to close up forming a coastal beach. This evolved into a large lagoon that was gradually filled in with sediments of continental origin. The marshlands are formed by two well differentiated layers with a high content in gravels and rounded material. Between these two layers and also on top of the most superficial layer, there are clays and clayey–sandy material.
e) Eolic mantle of stabilised and mobile sands. Stabilised sands are located in the NW part of the park (Clemente et al., 1997; Rodríguez Ramírez, 2008) as part of an old dune system showing variable thickness. Likewise, there is a small area of stabilised sands to the South, whose origin is the formation of bars and spits that allowed the filling up of the wetland, this area is almost at the same level as the high tide. Mobile sands are located in an area parallel to the coast line and consist in 3 or 4 mobile dune beaches, which can move up to 5 m/year (Clemente et al., 1997; Rodríguez Ramírez, 2008). Q4
f) Alluvial deposits. Recent sedimentary deposits on the floor and margins of rivers and streams.

From a tectonic point of view, the studies carried out (Benkhelil, 1976; Fernández et al., 1998; Rodríguez Vidal, 1989; Salvany and Custodio, 1995; Viguier, 1977) describe the zone as an area divided into blocks limited by the Guadalquivir fault and the lower Guadalquivir fault, Fig. 2. The onset of the superficial structures between those faults can be explained by a geotectonic tilt and by changes in the sedimentation environment (Salvany, 2004).

Q3

Please cite this article as: Martín, A., et al., A comparison of robust polynomial fitting, global geopotential model and spectral analysis for regional–residual gravity field separation in the Doñana National Park (Spain), J. Appl. Geophys. (2011), doi:10.1016/j.jappgeo.2011.06.037

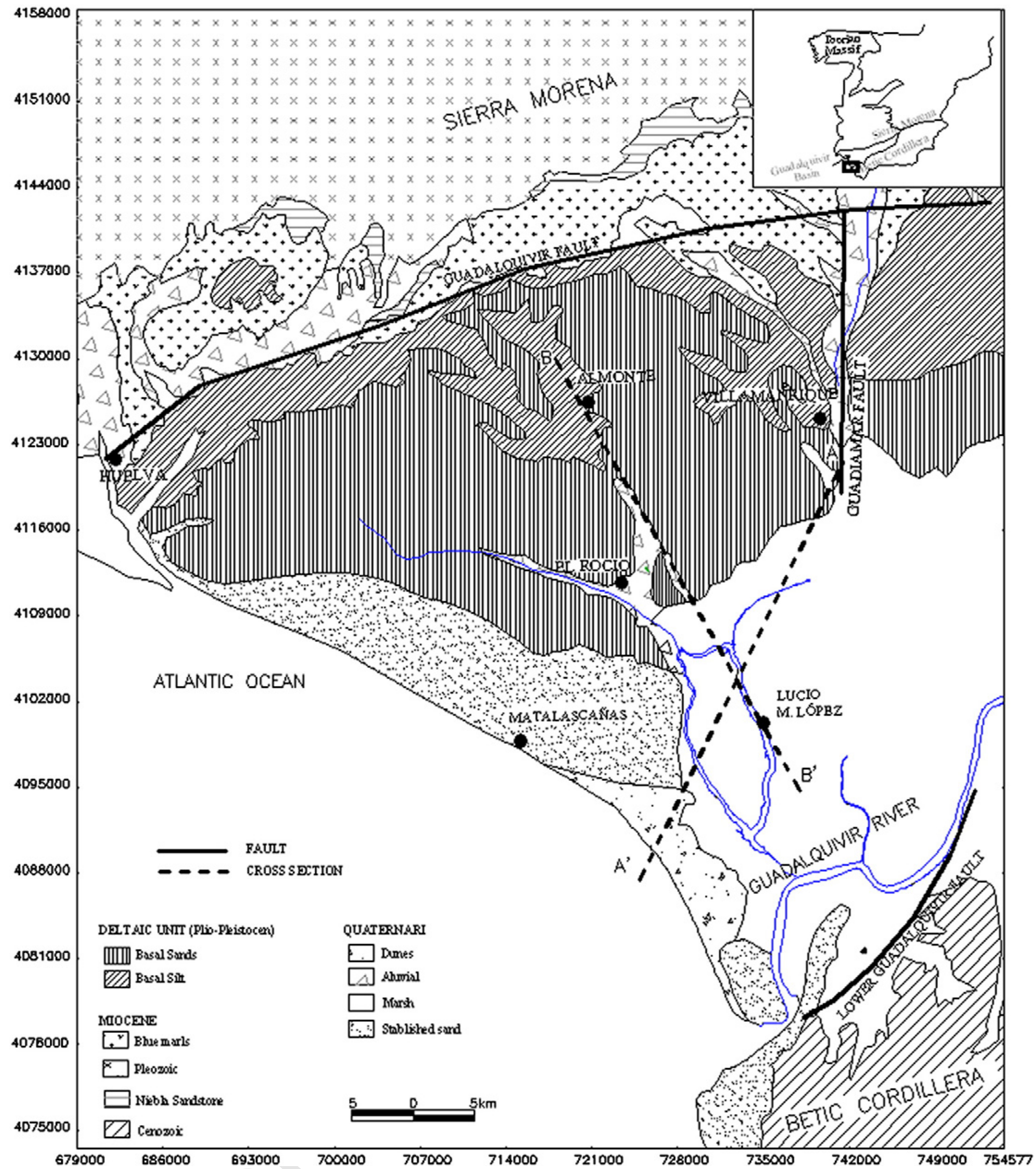

Q1 **Fig. 2.** Geology of the zone according to Montes et al., 1998; Salvany et al., 2001 and Salvany et al. 2004. UTM 29 N coordinates. GRS80 reference ellipsoid. Lucio is the local name for the lagoons inside the Park.

3. Data acquisition

3.1. Gravity data

82 gravity points, (Fig. 4), were observed with Lacoste & Romberg relative gravimeters, models D203, G301 and G1102. The measures are referenced to IGSN71 gravimetric datum by the inclusion of two known absolute gravity points (Sevilla B and Huelva B) of the Spanish Main Gravimetric Network (Sevilla et al., 1990) in the observation itineraries.

The data acquisition campaigns were carried out during the dry season, in July 1998, 2000, 2002, 2003, 2004 and October 2002. The gravimetric measures were corrected for tides, gravimeter height, presence of underground water, and drift (Torge, 1989). It is worth noting that the correction due to presence of water in the subsoil turned out to be insignificant. A pore volume between 15 and 20% and 1 m in the change of underground level during the gravimetric campaings have been used (Núñez, 2006), these values and the use of the Eq. (8.15) of Torge (2001) give a maximum value of 0.008 mGal. Repeated observations in Q5 different campaings over 11 gravimetric points have shown an agreement above 0.05 mGal. Despite Doñana National Park is a big area, there were significant limitations to have good gravity coverage due to the existence of large extensions of water, areas restricted for nesting or for protected species.

GPS receivers, (Trimble 4000 SSI, Trimble 4800 and Leica GS530), were used for planimetric positioning of the gravity data. The coordinates are referenced to the ETRF89 frame due to the use of 4 points of the national geodetic network REGENTE (Barbadillo and Quirós, 1996) in the differential static observations.

Finally, altimetric information was obtained using high-precision levelling (two digital levels were used) related to the national precision levelling network (N.A.P., which establishes the altimetric datum in Spain), in this particular case 3 points of the levelling between Huelva and Sevilla were used.

Please cite this article as: Martín, A., et al., A comparison of robust polynomial fitting, global geopotential model and spectral analysis for regional–residual gravity field separation in the Doñana National Park (Spain), J. Appl. Geophys. (2011), doi:10.1016/j.jappgeo.2011.06.037

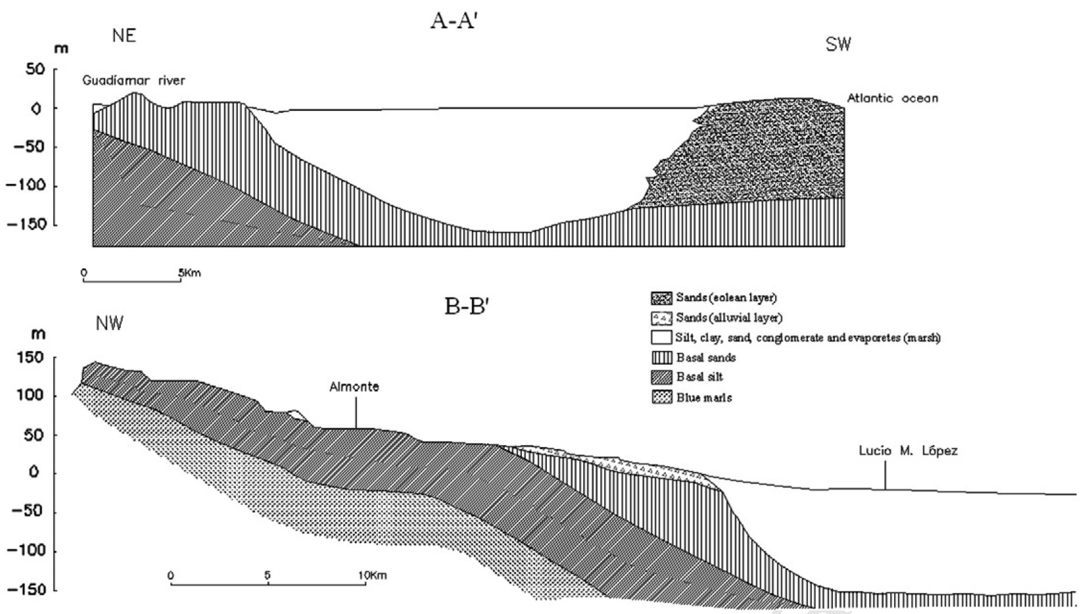

Fig. 3. Geological cross-sections, modified from IGTE, 1992, (see Fig. 2 for locations).

3.2. Digital model for elevations and depths

A digital elevation model is needed for Bouguer gravity anomalies computation. The digital elevation model used was produced by integrating the corresponding part of the Spanish National Geographic Institute (IGN) Digital Terrain Model at scale 1:25000 (referenced to Hayford's ellipsoid and to the mean sea level in Alicante) and the Spanish Marine Hydrographic Institute (IHM) 442 navigation chart (referenced to WGS84 ellipsoid and to the maximum low tide of the studied area). Due to the different geodetic reference system used in the two data set a unification has been done using a coordinate transformation (Núñez, 2004). The final digital elevation model covering the National Park is 62 km in NS direction and 42 km in EW direction, with a 25 × 25 m resolution and an accuracy better than 3 m. The geodetic reference system of this final model is Hayford's ellipsoid and the altimetric reference is the mean sea level, Fig. 5.

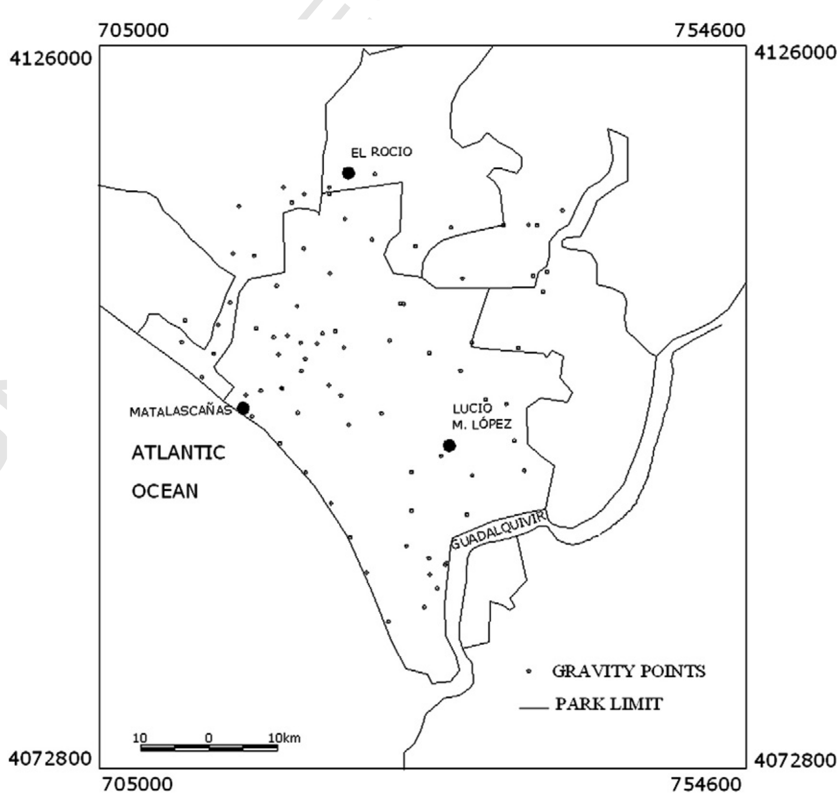

Fig. 4. Location of the observed gravity points. UTM 29 N coordinates. GRS80 reference ellipsoid.

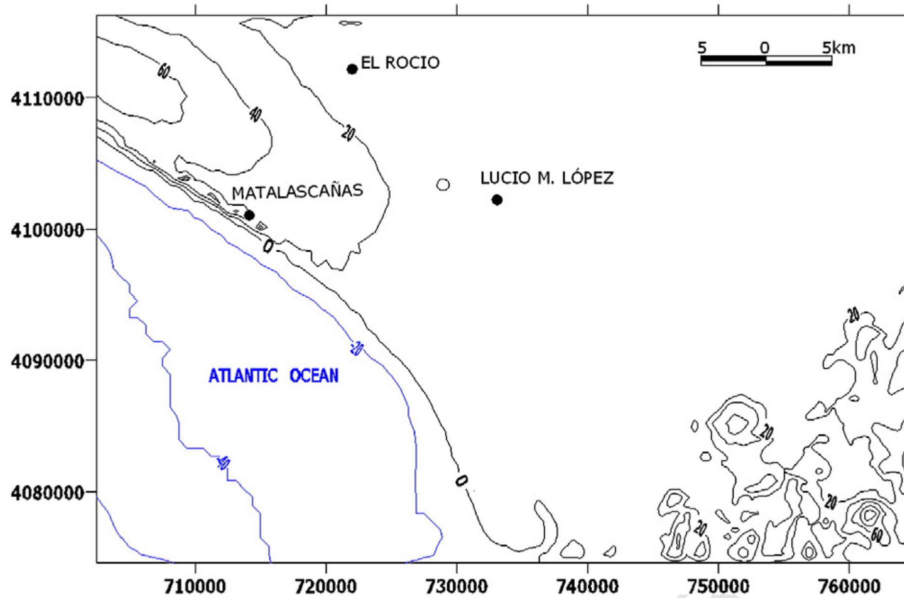

Fig. 5. Digital elevation and depths model. Mean: 4.8 m, max: 131 m, min: −40 m. UTM 29 N coordinates. GRS80 reference ellipsoid.

4. Bouguer gravity anomalies

Bouguer gravity anomalies were calculated with the usual expression (Heiskanen and Moritz, 1967), Fig. 8:

$$\Delta g^{Bouguer} = \Delta g^{Free-air} - B + C \tag{1}$$

C is the classical terrain correction, computed by rectangular prism integration method, taking into account the resolution of the digital elevation model (Forsberg and Tscherning, 1981), B is the Bouguer correction:

$$B = 2\pi K \rho H \tag{2}$$

where K is the universal gravitational constant, ρ is the crustal density (2.67 gr/cm^3) used in the Bouguer correction and H is the height of the point in metres, and the free-air anomalies ($\Delta g^{Free-air}$) were calculated using the following equation:

$$\Delta g^{Free-air} = g + 0.3086H - \gamma_O \tag{3}$$

where g expresses the observed gravity value and γ_O is the normal gravity value on the GRS80 reference ellipsoid computed using Somigliana formula.

Due to the small variations in elevation, Fig. 5, the maximum value for terrain correction is 0.089 mGal.

Table 1 presents a statistical summary of the Bouguer gravity anomalies obtained after gross-error detection and elimination as explained below, where the high gravity gradient in the area is clear, reaching values close to 40 mGal in less than 50 km.

Table 1
Statistical summary of the observed Bouguer gravity anomalies, the differences between the interpolated anomalies and their values for these points, and reduced Bouguer anomalies. Magnitudes in mGal.

	Mean (mGal)	σ (mGal)	Range (mGal)	Max. (mGal)	Min. (mGal)
Δg_{obs}	−9.684	11.803	42.987	10.679	−32.307
$\Delta g_{obs} - \Delta g_{int}$	0.012	1.907	12.469	5.521	−6.948
Δg^{Red}	2.345	2.186	9.527	7.911	−1.615

In order to completely validate the observed gravity, a method to found posible errors is performed (gross-error detection). This search is based on the interpolation of each gravity anomaly from the rest of the data (Δg_{int}) and their comparison with the observed value (Δg_{obs}). A point is thought to be prone to gross-error if the following equation applies, (Tscherning, 1991):

$$|\Delta g_{obs} - \Delta g_{int}| > k\left[\sigma_{int}^2 + \sigma_{obs}^2\right]^{\frac{1}{2}} \tag{4}$$

where k is a constant normally adopted as equal to 3, σ_{int}^2 is the error variance of the interpolation and σ_{obs}^2 is the error variance of the observations.

The most frequently method employed to interpolate data in many of the geodesic and geophysical applications is the least squares collocation method, (Moritz, 1980). The following expression is used in order to obtain the interpolated gravity anomaly at point P:

$$\Delta g_P = C_{Pi}\left(C_{ij} + C_e\right)^{-1}\Delta g_i \tag{5}$$

where C_{Pi} is the transposed covariance vector of the gravity anomaly between the calculation point P and points i, where the gravity anomaly was observed; C_{ij} is the covariance matrix between the points where the gravity anomaly was observed; C_e is the covariance diagonal error matrix of the observation points; and Δg_i is the observed gravity anomaly vector. The interpolation error variance can be calculated by means of the following expression, (Moritz, 1980):

$$\sigma_{(\Delta g)}^2 = C_{PP} - C_{Pi}\left(C_{ij} + C_e\right)^{-1} C_{Pi}^T \tag{6}$$

where C_{PP} is the variance of the gravity anomaly at point P.

In order to complete the above process, the covariance function should be defined. In this study, empirical covariance was calculated using the observed points (Knudsen, 1985). The following rule of thumb was used to obtain the optimum correlation step to determine empirical covariance (Tscherning and Forsberg, 1992):

$$e_d^2 = C_0\left(\frac{d0.3}{\psi}\right)^2 \tag{7}$$

where e_d is the desired mean error, equal to 0.05 mGal in agreement with the observed mean error obtained by repeated observations, C_0 and ψ are the variance and correlation distance respectively deduced from the empirical covariance distribution, and d is the correlation step. A correlation step of 0.018°, approximately 2 km, is obtained in order not to lose information. The empirical function, Fig. 6, has to be adjusted to a covariance model. Barzaghi et al. (1992) suggest various models of definite positive covariance functions, from which the selected function is (Camacho et al., 1997; Montesinos et al., 1999):

$$C(d) = C_0 J_0(cd) e^{-bd} \tag{8}$$

where J_0 is the zero-order Bessel function, C_0 is the variance of the empirical covariance distribution and b, and c are parameters calculated by an iterative least square adjustment to provide the best possible fit of function $C(d)$ to the empirical covariance values, and d is the distance.

As described in Camacho et al. (1994, 1997), once the gravity anomalies were calculated, the resulting residuals were considered for a second covariance analysis to detect, if possible, a secondary correlated signal in the gravity anomalies. Fig. 7 shows the empirical and adjusted covariance model, following the same procedure as before. The optimum correlation step is 0.011°. Note that this secondary signal is assumed to be uncorrelated noise, at least for the mean distance between gravity stations, so no further signal could be detected; therefore, only the first signal is used for interpolation.

By using this methodology, no point was found that would present gross errors. Table 1 presents a statistical summary of the Bouguer gravity anomalies where the high gravity gradient in the area is clear, reaching values close to 40 mGal in less than 50 km. The second row corresponds to the statistical summary of the results obtained when comparing the interpolated values and the observed values.

Once all the points observed are validated, the Bouguer gravity anomaly of any other point within the Doñana National Park can be obtained by using Eq. (5) and Eq. (6), the adjusted covariance function of Fig. 7 and the observed gravity anomalies.

5. Regional–residual gravity field separation

The existence of the Earth's gravitational field is a consequence of the superposition, within the crust, of masses with different densities. In general, this mass superposition is difficult to distinguish or identify individually. Terms such as "residual or local" and "regional" are often used to differentiate anomalies due to local causes close to the Earth's surface from deeper regional causes (Blakely, 1996; Dobrin and Savit, 1988; Sharma, 1997; Torge, 1989).

There are basically three methods for separating regional field from residual field:

- The adjustment of a polynomial to the gravitational field, assuming that a polynomial surface adequately models the field's regional component. The smoothness of the field is controlled by the polynomial degree, which should be low (see for instance, Camacho et al., 1994; Montesinos et al., 1999).
- The use of a global geopotential model to eliminate the field's low frequency component. The advantage of using this model is that it was obtained with actual gravity data gathered throughout the Earth (see for instance, Featherstone, 1997; Hackney et al., 2004).
- Spectral methods based on calculating the power spectrum of the gravitational signal and eliminating the low frequency components (see for instance, Ates and Kearey, 2000; Carbó et al., 2005; Chávez et al., 2007). This wavelength filtering can be used to emphasise or even reveal the existence of residual anomalies. High-pass filters, directional filters or the second vertical derivative are used to enhance short-wavelength components of the gravity field (Dobrin and Savit, 1988; Lodolo et al., 2007).

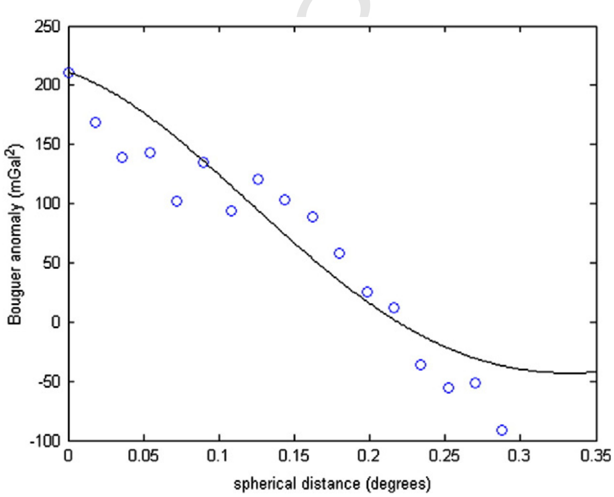

Fig. 6. Adjusted covariance function (line) and empirical covariance distribution (circles).

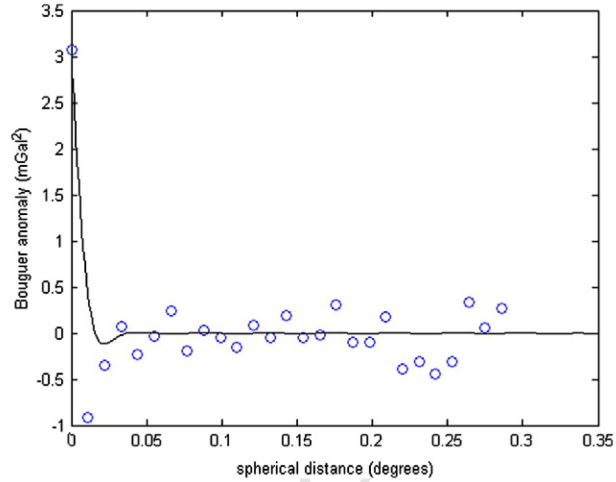

Fig. 7. Secondary adjusted covariance function (solid line) and empirical covariance distribution (circles).

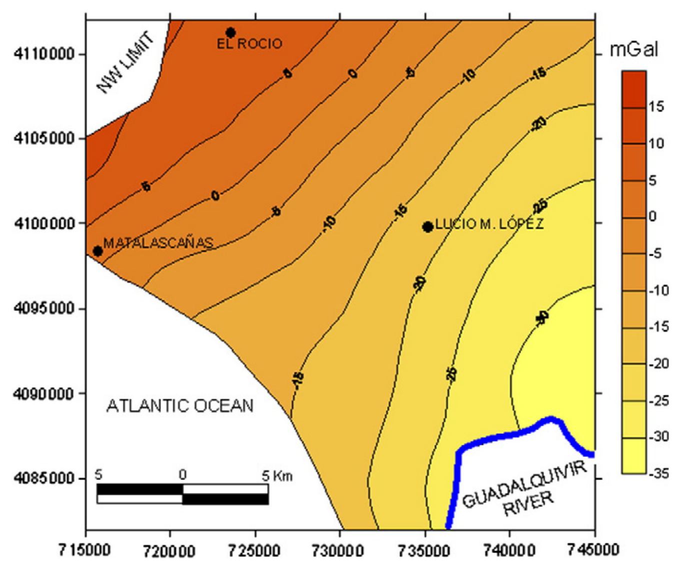

Fig. 8. Bouguer gravity anomalies. UTM 29 N coordinates. GRS80 reference ellipsoid. Units are mGal.

Please cite this article as: Martín, A., et al., A comparison of robust polynomial fitting, global geopotential model and spectral analysis for regional–residual gravity field separation in the Doñana National Park (Spain), J. Appl. Geophys. (2011), doi:10.1016/j.jappgeo.2011.06.037

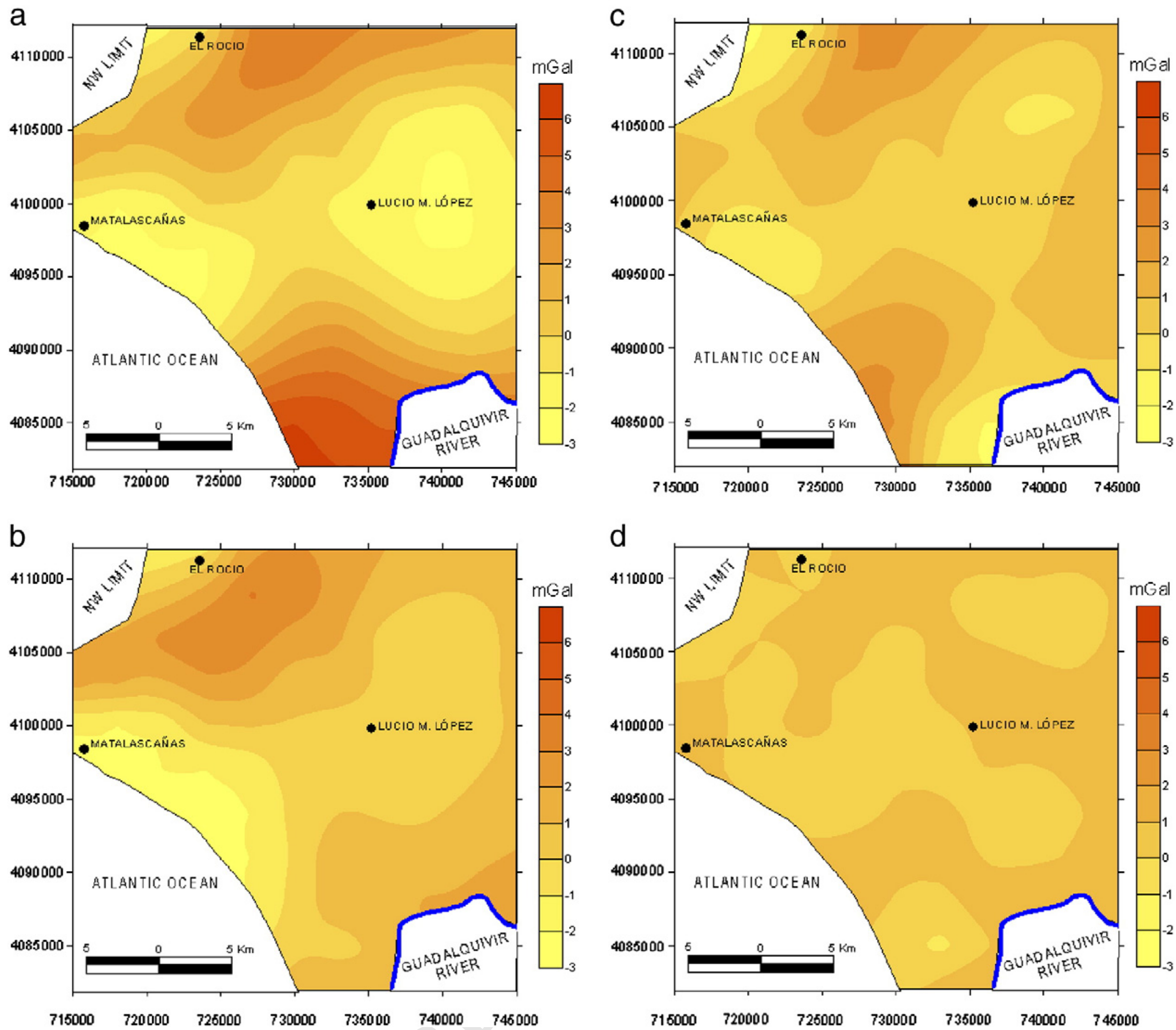

Fig. 9. a. Final residual gravity anomaly component of the first-order polynomial adjustment. UTM 29 N coordinates. GRS80 reference ellipsoid. Units are mGal. b. Final residual gravity anomaly component of the second-order polynomial adjustment. UTM 29 N coordinates. GRS80 reference ellipsoid. Units are mGal. c. Final residual gravity anomaly component of the third-order polynomial adjustment. UTM 29 N coordinates. GRS80 reference ellipsoid. Units are mGal. d. Final residual gravity anomaly component of the fourth-order polynomial adjustment. UTM 29 N coordinates. GRS80 reference ellipsoid. Units are mGal.

5.1. Low degree polynomial adjustment

Given the dimensions of the working area and taking into consideration the low gradient of the Bouguer anomalies (Fig. 8), it seems logical to use a low-degree polynomial for adjustment. The process is based on the progressive introduction of coefficients, that is, first, second, third, fourth, etc., degree polynomial adjustment should be done in that order. The result obtained after the substraction of the part corresponding to the polynomial adjustment to the original gravity data is the residual gravity signal. Fig. 9a shows the residual gravity field after first degree polynomial adjustment and elimination, and Fig. 9b, c, d after second, third and fourth degree polynomial adjustment and elimination, respectively. As can be seen, the adjustment to a fourth polynomial degree absorbs the major part of the gravity signal, so no residual signal can be found. Obviously the optimal polynomial to separate regional and residual gravity signal from the original data is the previous to that one which eliminates the major part of the total gravity signal, that is the third degree polynomial adjustment.

Fig. 10 shows the residual component of this third-order adjustment over the map of geological structures.

In order to obtain the coefficients for every polynomial (first, second, third and fourth degrees), a least square prediction was carried out using the robust polynomial fit described in Beltrao et al. (1991). This procedure is based on an iterative process that re-weights design matrix equations so that the weight w of a gravity observation i for iteration k will be:

$$w_i^k = e^{-t^2}, \quad if \quad t < 5.48, \tag{9a}$$

and

$$w_i^k = -0.1\left(\frac{t-5.48}{r_{max}}\right)^2, \quad if \quad t \geq 5.48, \tag{9b}$$

where $t = 0.6745 r_i^{(k-1)}/s^{(k-1)}$, r_{max} is the maximum absolute residue in iteration $(k-1)$, $s^{(k-1)}$ is the mean of the absolute residues of iteration $(k-1)$. Constant 0.6745 causes $s^{(k-1)}$ to become a consistent predictor of standard deviation if Gaussian noise-contaminated observations are presented. Value 5.48 is chosen as it practically corresponds to the null weight of Eq. (9a). For the first iteration, the weight vector value is the result of estimated observation error, obtained by repeated field measurements at the same points. With this method the best coefficients for each polynomial are obtained.

Please cite this article as: Martín, A., et al., A comparison of robust polynomial fitting, global geopotential model and spectral analysis for regional–residual gravity field separation in the Doñana National Park (Spain), J. Appl. Geophys. (2011), doi:10.1016/j.jappgeo.2011.06.037

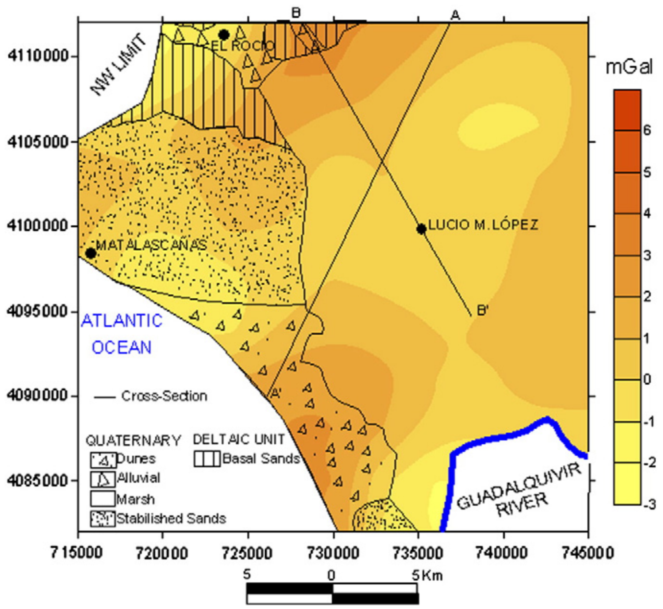

Fig. 10. Residual gravity anomaly component of the third-order polynomial adjustment. UTM 29 N coordinates. GRS80 reference ellipsoid. Units are mGal.

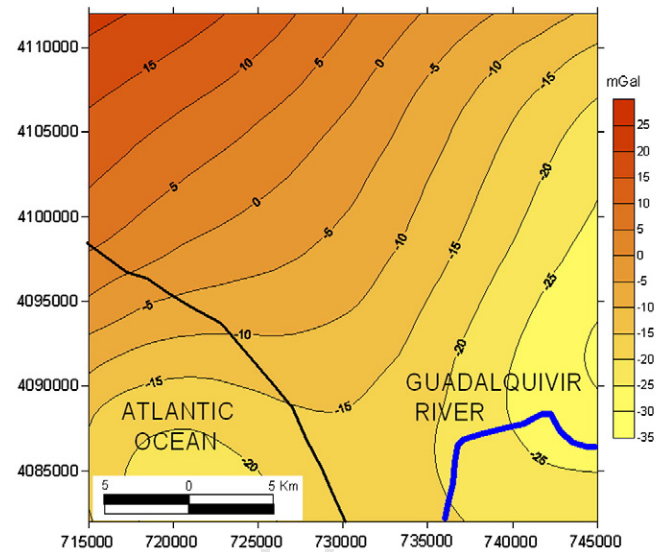

Fig. 11. Gravity anomalies of the EGM2008 global geopotential model. UTM 29 N coordinates. GRS80 reference ellipsoid. Units are mGal.

5.2. Use of a global geopotential model

Since the launch of the CHAllenging Minisatellite Payload (CHAMP) and Gravity Recovery and Climate Experiment (GRACE) missions (2000 and 2002, respectively), more than 25 new global geopotential models (GGM) have become available to the scientific community through the public domain http://icgem.gfz-potsdam.de/ICGEM. These models lead to significant improvement of our knowledge of the long wavelength part of the Earth's static gravitational field, so can be used for regional–residual gravity field separation. Since 2004, the United States National Geospatial-Intelligence Agency (NGA) has embarked upon the development of a new Global Geopotential Model (GGM) of very high degree and order (Pavlis et al., 2004). This new model is the EGM2008 (Pavlis et al., 2008), complete up to degree and order 2159. It also has additional coefficients up to degree 2190 and order 2159, recovering the gravitational field up to 20 km wavelengths. EGM2008 is based on the following data sets: a new $5' \times 5'$ gravity database for the entire planet provided by the National Geospatial-Intelligence Agency, data from the GRACE satellite mission (ITG-GRACE03S geopotential model, Mayer-Gürr, 2007, along with its complete error covariance matrix, was used), a new elevation database based on the Shuttle Radar Topographic Mission solution along with other databases (GTOPO30, ICESat, etc.), and the new mean sea surface using data from the Topex/Poseidon, Jason-1, ERS-1/2, Geosat, Envisat, GFO and ICESat altimetric satellites.

The standard deviation of gravity anomaly is better than 3 mGal in the research area, Pavlis and Saleh, 2005, http://earth-info.nima.mil/GandG, and can be considered as a constant due to the small dimensions of the studied area. Fig. 11 is a plot of EGM2008 GGM, whilst Fig. 12 shows the reduced gravity field, namely the result of eliminating the gravity anomalies of the global model from Bouguer gravity anomalies, on the map of geological structures. This reduced gravity field corresponds to the residual gravity component in the regional–residual gravity field separation schema defined in this paper. Table 1 shows the statistical summary of the residual anomalies where the range of anomalies reduces significantly compared with the original Bouguer anomalies.

5.3. Signal filtering

In order to achieve Fourier's analysis, Bouguer anomalies should be interpolated to a grid. This interpolation was carried out using Eq. (5) and Eq. (6). The optimum grid spacing between nodes should be carefully studied. It is of no value to create a much finer grid than the one justified by the original data distribution and quality, so the grid spacing of 2×2 km, as Eq. (7) indicates, has been used. The statistical summary of the Bouguer anomalies can be seen in Table 2.

The mean radial power spectrum of gravity data can be divided, in general, into three segments (Carbó et al., 2005; Chávez et al., 2007; Q9 Grupta and Ramani, 1980). The part at the long wavelength with a steep slope is assigned to the regional gravity signal (sources that are deep and/or broad). The short wavelengths, with flatter slope, are assigned to the residual gravity signal (relatively shallow sources). At very high frequencies, the spectrum is dominated by the effects due to measurement errors, gridding errors, etc.

Fig. 13 presents the mean radial power spectrum of the Bouguer anomaly grid. As can be seen two linear segments of differentiated slope can be recognised, the separation of these two segments is situated at the 15 km wavelength, but we cannot conclude that this is the wavelength for regional–residual potential field separation because,

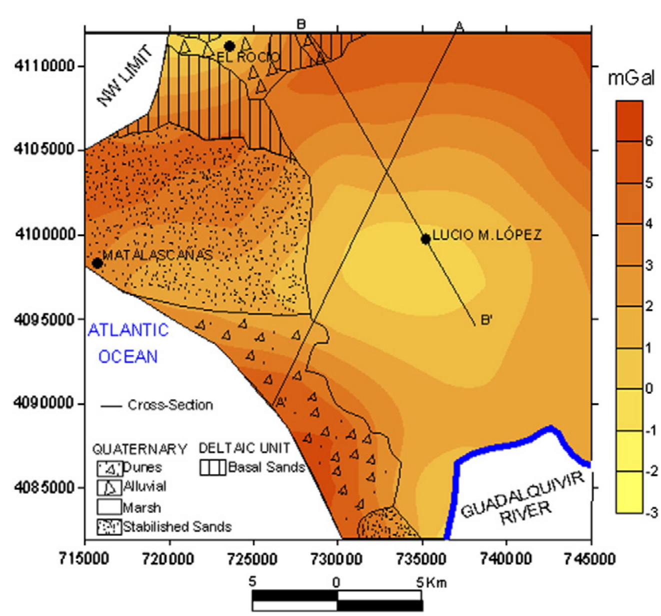

Fig. 12. Reduced (residual) Gravity anomalies of the EGM2008 global geopotential model. UTM 29 N coordinates. GRS80 reference ellipsoid. Units are mGal.

Table 2
Statistical summary of the Bouguer anomalies (Δg) and reduced Bouguer anomalies (Δg^{Red}) calculated on a 2×2 km grid and the associated error. Magnitudes in mGal.

	Mean (mGal)	σ (mGal)	Range (mGal)	Max. (mGal)	Min. (mGal)
Δg_{int} (grid)	−11.874	12.334	45.044	12.603	−32.440
$\sigma_{\Delta gint}$ (grid)	3.322	2.782	10.442	10.457	0.015

first of all, the regional field has much larger wavelengths than what can be recovered in the studied area, usually maximum recoverable wavelength is about 25-40 km (Carbó et al., 2005; Chávez et al., 2007; Grupta and Ramani, 1980), and secondly, it is well known that deep seated sources cannot produce short wavelength fields, however large shallow structures can produce long wavelengths, so the wavelengths over 15 km correspond to the wavelengths of local (residual) sedimentary structures, which are the principal structures identified in the polynomial regional–residual separation as can be concluded from Figs. 14 and 15, which show the mean radial power spectrum of the residual gravitational field for the third order polynomial adjustment on Bouguer anomalies and residual Bouguer anomalies from EGM2008 GGM respectively. These power spectrum plots are quite similar to the power spectrum plot in Fig. 13: the two differentiated segments are shown with a separation at the 12 km wavelength in Fig. 14 and at the 15 km wavelength in Fig. 15, indicating that the same features are present in the Bouguer anomalies and in the residual (third order or EGM2008) Bouguer anomalies, that is, a part of the residual gravity signal.

Finally these sedimentary structures, located at the long wavelengths (from 15 km), cannot be separated from the original signal because the cutting wavelength is nearly half the size of the area. Therefore, the coefficients of the longer wavelengths are not well determined by a Fourier analysis which may lead to relatively large uncertainties in the filter outcome.

The only certain point is that noisy cut off is located in the lower part of the spectrum (12–15 km.), which is the same wavelength obtained in other works (Carbó et al. 2003 and Chávez et al., 2007 for example).

In conclusion, signal filtering can not be done here simply because the recovered area is too small.

6. Interpretation of residual anomalies

Residual gravity anomalies related to the third-order polynomial adjustment, (Fig. 11) shows a low density area (low gravity anomaly values, with regard to neighbouring values) that crosses the centre of the park from NE to W. This low-density area corresponds to low density sediments from the Marshlands in the NE area and, in the W, it is situated between the eolic mantle of mobile sands (dunes) and stabilised sands. The alluvial deposits situated at the NW part of the park generate a low relative density area, Fig. 2 and, finally the low relative density area in the South corresponds to the southern settlement of stabilised sands or old beach, whose low density value is due to its location at high tide level, Fig. 2. The high relative density area located in the SW corresponds to the eolic mantle of mobile sands (dunes), and, finally, the relative high density feature located at the N, crossing from N to NW, are related to the basal sands.

Fig. 12 (residual gravity anomalies related to EGM2008 GGM), shows the same behaviour as Fig. 10, but with high marked trends, related in particular to the high relative density area of the eolic mantle of mobile sands and the basal sands that completely cross the research area from NE to NW (except for the low density anomalies related to the alluvial deposit). These marked trends, compared to Fig. 10, can be clearly found in Fig. 16 and Fig. 17, where the two cross-sections are reproduced (Fig. 3) with the residual gravity values of the profiles plotted. The slopes of the EGM2008 residual gravity profile are higher than the residual gravity profile of the third-order adjustment. This is expected due to the omission error of EGM2008, which generates signal in the residual gravity anomalies from more deeper sources than the third-order polynomial adjustment. But both

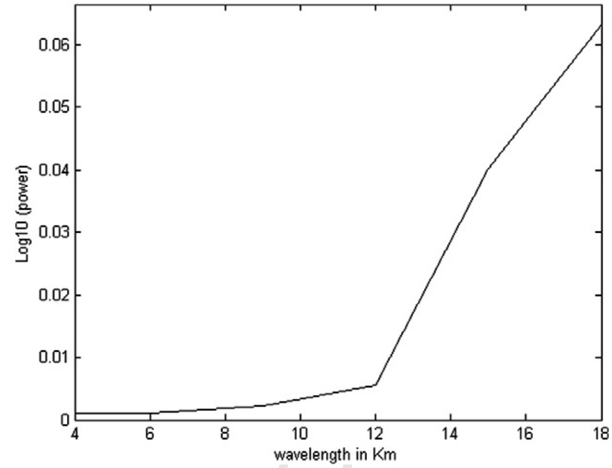

Fig. 14. Radial-averaged power spectrum of the residual gravitational field for the third-order polynomial adjustment on Bouguer anomalies.

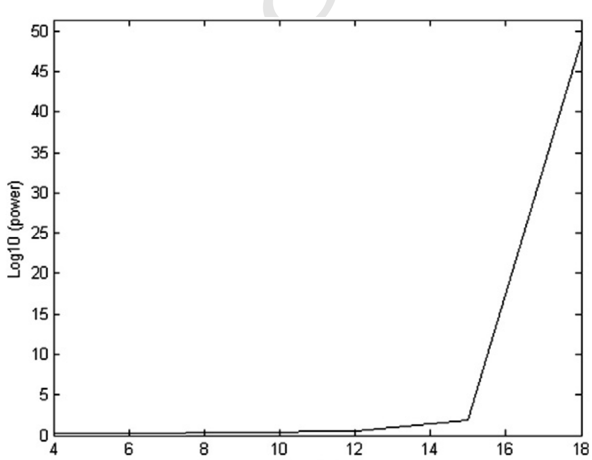

Fig. 13. Radial-averaged power spectrum of Bouguer anomaly map. Units are mGal.

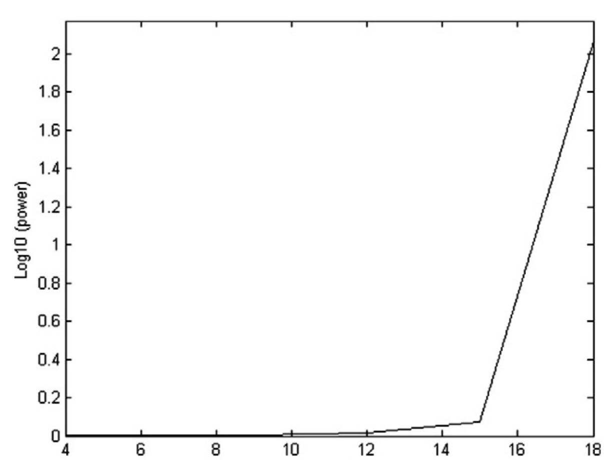

Fig. 15. Radial-averaged power spectrum of the residual gravitational field from EGM2008 GGM.

Please cite this article as: Martín, A., et al., A comparison of robust polynomial fitting, global geopotential model and spectral analysis for regional–residual gravity field separation in the Doñana National Park (Spain), J. Appl. Geophys. (2011), doi:10.1016/j.jappgeo.2011.06.037

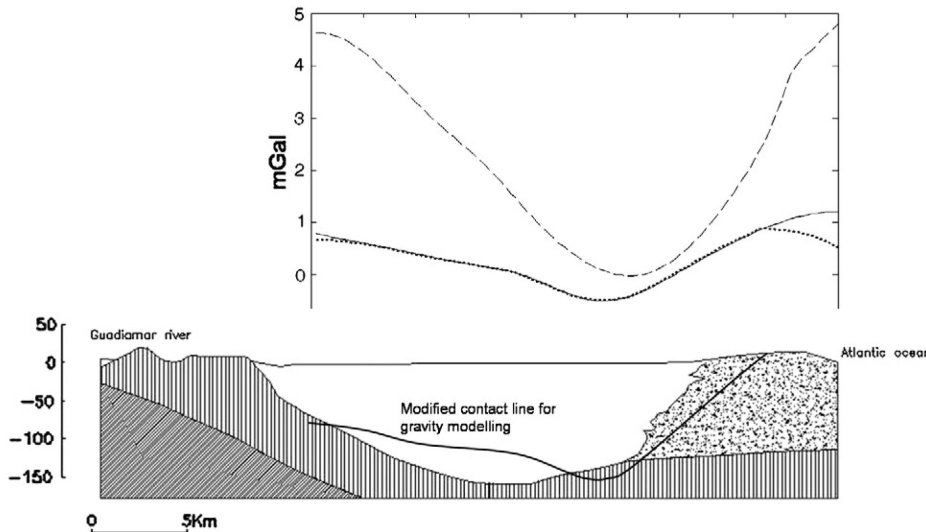

Fig. 16. Geological cross-section AA′ of Fig. 2 with the computed residual gravity anomalies from EGM2008 (dashed line) and from third-order polynomial adjustment. Dots line corresponds to the modelled gravity of the geological features.

gravity profiles in the two sections have the same behaviour: for the AA′ cross-section low relative density values in the marshlands and high relative density values related to basal sands in the NE area and mobile sands in the W area can be found and for the BB′ cross-section the low relative density values related to the marshlands and the high relative density values related to the basal sands can be observed. Finally, these figures show that the above interpretations are not only due to lateral density variations, but also to thickness variations.

In order to check the geometry and density of the geological features, gravity profiles (Fig. 16 and Fig. 17) were modelled. The measure of materials' density is quite difficult due to the imposibility to obtain a good value for the volume of the material in a borehole: everything is detached material (sand, silt, clay) that collapse during the extraction process. So a mean value for sands (2.3 gr/cm^3) was assigned for basal sands, eolean sands (dunes) and alluvial sands, 2.0 gr/cm^3 for the materials of the marsh (which is the mean density for unconsolidated sediments (Buger, 1992)) and 2.4 gr/cm^3 for basal silt. The modelling was carried out with the GravModeler software, which performs 2D modelling of gravity data based on the line integral approach of the classical Talwani method (Talwani et al., 1959) using bodies of various densities embedded within a homogeneous background. The separation line between the 2.3 gr/cm^3 structures and the marsh in the two cross-sections has been modified in order to give the best approximation fitting to the residual gravity anomalies produced by the third-order polynomial adjustment. Some differences between modelled and observed gravity can be found in the limits of the profiles due to the software treatment of the vertices as infinitely far to the left and right.

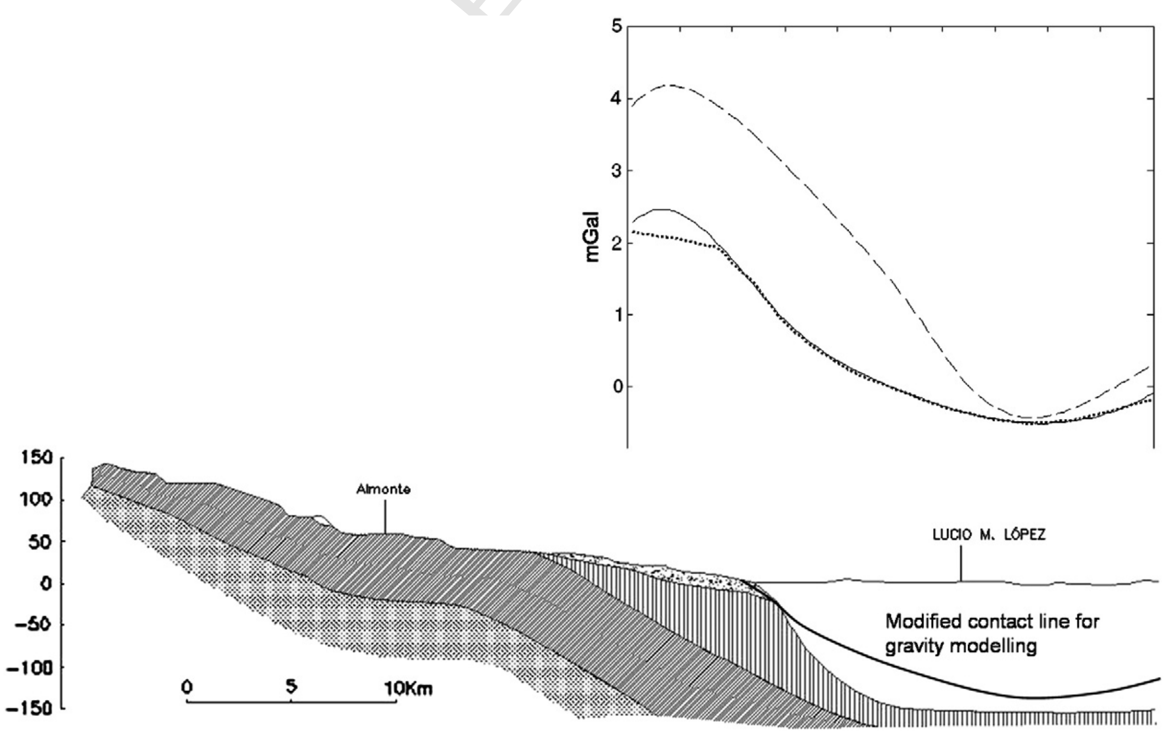

Fig. 17. Geological cross-section BB′ of Fig. 2 with the computed residual gravity anomalies from EGM2008 (dashed line) and from third-order polynomial adjustment. Dots line corresponds to the modelled gravity of the geological features.

7. Conclusions

In order to carry out the gravimetric study of the Doñana National Park and draw some geological conclusions, the regional component must be separated from the residual one within the gravitational signal. This separation was obtained by means of a third-order polynomial adjustment to the Bouguer gravity anomalies and the use of the EGM2008 global gravitational model.

The results concluded that the residual anomalies obtained from third-order adjustment or from EGM2008 GGM are equivalent, showing the great possibilities of the very-high degree global geopotential model EGM2008 for gravimetric studies and regional–residual gravity field separation. Nevertheless it is not possible to conclude which is the best suited method to perform a correct regional–residual separation, in any case the use of, at least, two of them (including spectral methods) are highly recommended.

The interpretation of the results is justified by the well-known geological aspects of the park: low relative density areas are related to the Marshlands, alluvial deposits and the old beach whilst high relative density areas are related to the variability of thickness of the dunes and basal sands. The most important differences between geology and residual gravity field are related to the modification of some boundaries for a correct modelling of the cross-sections, partly due to the distance between gravity observations and partly due to a possible bad identification of the specific precise limits of the geological structures within the Park.

Acknowledgements

The studies presented here were part of CICYT (Spanish Research Directorate) research project nos. HID 97-0321 and REN2001-1293. We would like to thank all UPC members participating in these projects and the staff from the Biological Station of Doñana (CSIC), Palacio de Doñana and Doñana National Park. We remain deeply grateful for the fruitful discussion with Dr. Salvany and for the geological review of the manuscript.

We gratefully acknowledge the cooperation in the form of technical and material support from the Geodesic and Geophysical departments of the National Geographic Institute (IGN), the Institut Cartogràfic de Catalunya (ICC), the Seville Port Authority, the Guadalquivir River Water Authority (CHG) and the Technical University of Valencia. Likewise, we are grateful for the levelling data of J.A. Mintegui and J.C. Robredo (ETSIM-UPM).

Finally, we are grateful for the efforts of reviewers and editor whose comments have helped improved the manuscript.

References

Ates, A., Kearey, P., 2000. Interpretation of gravity and aeromagnetic anomalies of the Kenya region, south central Turkey. Journal of the Balkan Geophysical Society 3 (3), 37–44.

Barbadillo, A., Quirós, R., 1996. Proyecto REGENTE. Una nueva Red Geodésica Nacional. Física de la Tierra. Geodesia y Geofísica 8, 23–38 (in Spanish).

Barzaghi, A., Gandino, A., Sanso, F., Zenucchini, C., 1992. The collocation approach to the inversion of gravity data. Geophysical Prospecting 40, 429–451.

Beltrao, J.F., Silva, J.B.C., Costa, J.C., 1991. Robust polynomial fitting method for regional gravity estimation. Geophysics 56 (1), 80–89.

Benkhelil, J., 1976. Etude néotectonique de la terminaison occidentale des cordillères Bétiques, Thèse, Université de Nice, (in French).

Blakely, R.J., 1996. Potential theory in gravity and magnetic applications. Cambridge Univ. Press.

Buger, H.R., 1992. Exploration Geophysics of the Shallow Subsurface. Prentice Hall PTR.

Camacho, A.G., Vieira, R., Montesinos, F.G., Cuellar, V., 1994. A gravimetric 3D global inversion for cavity detection. Geophysical Prospecting 42, 113–130.

Camacho, A.G., Montesinos, F.G., Vieira, R., 1997. A three-dimentional gravity inversion applied to Sao Miguel Island (Azores). Journal of Geophysical Research 102 (B4), 7717–7730.

Carbó, A., Muñoz-Martín, A., Llanes, P., Álvarez, J., EEZ Working Group, 2005. Gravity analysis offshore the Canary Islands from a systematic survey. Marine Geophysical Researches 24, 113–127.

Chávez, R.E., Flores-Márquez, E.L., Suriñach, E., Galindo-Zaldivar, J.G., Rodríguez-Fernández, J.R., Maldonado, A., 2007. Combined use of the GGSFT data base and on board marine collected data to model the Moho beneath the Powell Basin Antarctica. Geological Acta 5 (4), 323–335.

Clemente, L., Siljeström, P., Rodríguez-Ramírez, A., 1997. Relación suelo/geomorfología en el Parque Nacional de Doñana. Cuaternario y Geomorfología 11 (1–2), 33–41 (in Spanish).

Dobrin, M.B., Savit, C.H., 1988. Introduction to Geophysical Prospecting, Fourth edition. McGraw-Hill, Inc.

Featherstone, W.E., 1997. On the use of the geoid in geophysics: a case study over the North-East shelf of Australia. Exploration Geophysics 28 (1), 52–57.

Fernández, M., Berasategui, X., Puig, C., García-Castellanos, D., Jurado, M.L., Torné, M., Banks, C., 1998. Geophysical and geological constraints on the evolution of the Guadalquivir foreland basin, Spain. Geological Society Special Publication 134 (4), 29–48.

Forsberg, R., Tscherning, C.C., 1981. The use of height data in gravity field approximation by collocation. Journal of Geophysical Research 86 (B9), 7843–7854.

García-Castellanos, D., Fernández, M., Torné, M., 2002. Modeling the evolution of the Guadalquivir foreland basin (Southern Spain). Tectonics 21 (3), 1–17. doi:10.1029/2001TC001339.

Grupta, V.K., Ramani, N., 1980. Some aspects of regional–residual separation of gravity anomalies in Precambrian terrain. Geophysics 45 (9), 1412–1426.

Hackney, R.I., Featherstone, W.E., Götze, H.L., 2004. Regional–residual gravity field separation in the central Andes using global geopotential models. Extended abstracts of the ASEG 17th Geophysical Conference and Exhibition, Sydney. .

Heiskanen, W.A., Moritz, H., 1967. Physical Geodesy. W.H. Freeman, San Francisco.

Instituto Tecnológico Geominero de España, ITGE, 1992. Hidrogeología del Parque Nacional de Doñana y su entorno. Colección de informes de aguas subterráneas y geotecnia. Editado por ITGE, Madrid (in Spanish.

Knudsen, P., 1985. Estimation and modelling of the local empirical covariance function using gravity and satellite altimeter data. Bulletin Géodésique 61, 145–160.

Lodolo, E., Lippai, H., Tassone, A., Zanolla, C., Menichetti, M., Hormaechea, J.L., 2007. Gravity map of The Isla Grande de Tierra del Fuego and morphology of Lago Fagnano. Geologica Acta 5 (4), 307–314.

Mayer-Gürr, T., 2007. ITG-GRACE03S: the latest GRACE gravity field solution computed in Bonn. Joint International GSTM and DFG SPP symposium. 15-17 October 2007, Potsdam.

Montes, C., Borja, F., Bravo, M.A., Moreira, M., 1998. Reconocimiento biofísico de los espacios naturales de Andalucía. CMA, Junta de Andalucía, Sevilla. . (in Spanish).

Montesinos, F.G., Camacho, A.G., Vieira, R., 1999. Análisis of gravimetric anomalies in Furnas Caldera (Sao Miguel, Azores). Journal of Volcanology and Geothermal Research 92, 67–81.

Moritz, H., 1980. In: Wichmann Verlag, Karlsruhe (Ed.), Advanced Physical Geodesy.

Núñez, A., 2004. Analysis of digital elevations models in National Park of Doñana (Spain). Proceedings GGSM2004, Oporto. August-September, 2004.

Núñez, M.A., 2006. Determinación de un geoide de precisión en áreas de pequeña extensión. Aplicación en el Parque Nacional de Doñana (in Spanish). Doctoral Thesis. Departamento de Ingeniería del Terreno, Cartografía y Geofísica. Universidad Politécnica de Cataluña. Spain. 329 pp. (in Spanish).

Núñez, M.A., Martín, A., Gili, J.A., Anquela, A.B., 2008. High-precision geoid determination in small areas: a case study in Doñana National Park (Spain). Studia Geophysica et Geodaetica 52, 361–380.

Pavlis, N.K., Saleh, J., 2005. In: Jekeli, et al. (Ed.), Error propagation with geographic specificity for very high degree geopotential models. : Gravity, Geoid and Space Missions, IAG symposia, 129. Springer-Verlag, Berlin.

Pavlis, N.K., Holmes, S.A., Kenyon, S.C., Schmidt, D., Trimmer, R., 2004. A preliminary gravitational model to degree 2160. IAG International Symposium GGSM2004, Oporto, Portugal.

Pavlis, N.K., Holmes, S.A., Kenyon, S.C., Factor, J.K., 2008. An Earth gravitational model to degree 2160: EGM2008. European Geosciences Union General Assembly 2008, Vienna, Austria.

Rodríguez Ramírez, A., 2008. Geomorfología del Parque Nacional de Doñana. Facultad de Ciencias Experimentales: Geología de Huelva, Lugares de Interés Geológico. Huelva University.

Rodríguez Vidal, J., 1989. La evolución neotectónica del Sector Occidental de la Depresión del Guadalquivir en el Cuaternario en Andalucía Occidental. AEQUA Monografías 1, 21–26 (in Spanish).

Salvany, J.M., 2004. Tilting neotectonics of the Guadiamar drainage basin, SW Spain. Earth Surface Processes and Landforms 29, 145–160.

Salvany, J.M., Custodio, E., 1995. Características litoestratigráficas de los depósitos pliocuaternarios del bajo Guadalquivir en el área de Doñana: implicaciones hidrogeológicas (in Spanish). Revista de la Sociedad Geology España 8, 21–31 (in Spanish).

Salvany, J.M., Mediavilla, C., Mantecón, R., Manzano, M., 2001. Geología del valle del Guadiamar y áreas colindantes. Boletín Geológico y Minero 57–68 (in Spanish).

Sevilla, M.J., Gil, A.J., Romero, P., 1990. Adjustment of the first order gravity net in the Iberian Peninsula. Bureau Gravimétrique Internacional Bulletin d'Information 66, 21–54.

Sharma, P.V., 1997. Environmental and Engineering Geophysics. Cambridge University Press.

Talwani, M., Worzel, J.L., Landisman, M., 1959. Rapid gravity computations for two-dimensional bodies with application to the Mendocino submarine fracture zone. Journal of Geophysical Research 64 (1), 49–61.

Torge, W., 1989. In: Walter de Gruyter (Ed.), Gravimetry. Berlín-New York.

Tscherning, C.C., 1991. A strategy for gross-error detection in satellite altimeter data applied in the Baltic-sea area for enhanced geoid and gravity determination. In: Rapp, R.H., Sansó, F. (Eds.), Determination of the geoid. : Present and Future, IAG Symposia 106. Springer, Berlin, Heidelberg, New York, pp. 95–107.

Tscherning, C.C., Forsberg, R., 1992. Harmonic continuation and gridding effects on geoid height prediction. Bulletin Géodésique 66, 41–53.

Viguier, C., 1977. Les grands traits de la tectonique du bassin néogène du Bas-Guadalquivir. Boletín Geológico y Minero 88 (1), 39–44 (in French).

Please cite this article as: Martín, A., et al., A comparison of robust polynomial fitting, global geopotential model and spectral analysis for regional–residual gravity field separation in the Doñana National Park (Spain), J. Appl. Geophys. (2011), doi:10.1016/j.jappgeo.2011.06.037